Application of Subspace State-space Identification Methods on Actuated Multibody Systems

Mathias Marquardt*, Peter Dünow*, Sandra Baßler* and Frank Wobbe†
Email: mathias.marquardt@hs-wismar.de
* Hochschule Wismar - University of Technology, Business and Design, Wismar, Germany
† IAV GmbH - Ingenieurgesellschaft Auto und Verkehr, Berlin, Germany

***Abstract*—In the last years subspace-based system identification methods have been developed for the application in open and even closed loop conditions. In this paper some of those methods are selected and applied to a nonlinear mechanical system in order to identify a local linear state space description of the underlying system. The considered plant is an actuated multibody system with two inputs and two outputs. The nonlinear nature of such a system leads to unstable behavior in some operating conditions so the system has to be operated in closed loop control during the identification procedure too. Considering these demands for the process of system identification the capability of subspace-based methods to identify stable and unstable MIMO systems using input-output data obtained from closed loop control experiments is investigated.**

I. Introduction

For data based modeling of systems prediction error methods (PEM) [6] and subspace state space identification (SSID) were developed over the years. When it comes to identification of multiple input multiple output (MIMO) systems subspace identification has major advantages over PE methods, since it can easily be extended for MIMO systems. Other advantages of subspace methods are the none iterative behavior and the possibility of optimal order selection as an intermediate step of the algorithm.

In the beginning of subspace model identification the algorithms could only be used on input-output data obtained from open loop experiments in order to get unbiased estimates of the system, because of the correlation between future input and past innovation data [5]. To overcome this problem different methods emerged which have modified the existing open loop subspace identification procedures such as Numerical Subspace State Space System IDentification (N4SID) [4], Canonical Variate Analysis (CVA) [1] and MIMO Output-Error State Space model identification (MOESP) [3] to give unbiased estimates even with measurement data obtained under closed loop conditions.

Ljung and McKelvey [5] suggested pre-estimating of a high order ARX model and using it to construct a j-step ahead predictor which is unbiased if there is at least one step delay between the plant output and the control input. This approach was later used for example by Chiuso [9] for the class of predictor based subspace identification (PBSID). Another approach of using the high order ARX model is for estimating an innovation sequence which was proposed by Qin and Ljung [8].

These algorithms were combined in a unified framework by de Korte [10] and classified in single-stage, double-stage and multi-stage class of algorithms. In this paper three algorithms of this unified framework - one of each class - are described and used for identification of a two by two MIMO mechanical system.

In this paper several subspace state space identification methods are first discussed in section II and in advance applied on an actuated multibody system in closed loop control condition in section III and IV. Section V gives some results of the performed experiments.

II. Subspace state space identification

In this section the used subspace state space identification algorithms are explained. The model considered for identification is the following state space model and it is common for all three algorithms:

$$\boldsymbol{x}_{k+1} = \mathbf{A}\boldsymbol{x}_k + \mathbf{B}\boldsymbol{u}_k + \mathbf{K}\boldsymbol{e}_k \tag{1}$$

$$\boldsymbol{y}_k = \mathbf{C}\boldsymbol{x}_k + \mathbf{D}\boldsymbol{u}_k + \boldsymbol{e}_k \tag{2}$$

with $\mathbf{A} \in \mathbb{R}^{n\times n}$ the system matrix, $\mathbf{B} \in \mathbb{R}^{n\times m}$ the input matrix, $\mathbf{C} \in \mathbb{R}^{l\times n}$ output matrix and $\mathbf{D} \in \mathbb{R}^{l\times m}$ feedthrough matrix. $\mathbf{K} \in \mathbb{R}^{n\times l}$ is the Kalman gain. $\boldsymbol{x}_k \in \mathbb{R}^n$, $\boldsymbol{u}_k \in \mathbb{R}^m$, $\boldsymbol{y}_k \in \mathbb{R}^l$ and $\boldsymbol{e}_k \in \mathbb{R}^l$ are the state, input, output and innovation vectors, respectively. Furthermore $\mathbf{e}_k$ is a zero-mean white Gaussian noise signal with the covariance $\mathbf{R}$ (3), where δ_{ij} is the Kronecker delta.

$$E(\mathbf{e}_i\mathbf{e}_j^T) = \mathbf{R}\delta_{ij} \tag{3}$$

Before explaining the algorithms in detail some notations and formulations have to be declared. The data block Hankel matrices have the following notation:

$$\mathbf{Y}_{k,\tau,\sigma} = \begin{bmatrix} \boldsymbol{y}_k & \cdots & \boldsymbol{y}_{k+\sigma-1} \\ \vdots & \ddots & \vdots \\ \boldsymbol{y}_{k+\tau-1} & \cdots & \boldsymbol{y}_{k+\tau+\sigma-2} \end{bmatrix} \tag{4}$$

So to build "'past"' and "'future"' data Hankel matrices from input and output measurement data the notation is $\mathbf{Y}_p = \mathbf{Y}_{0,p,N}$ for past data and $\mathbf{Y}_f = \mathbf{Y}_{p,f,N}$ for future data. The notation is the same for the input data $\mathbf{U}_p, \mathbf{U}_f$ and the innovation data $\mathbf{E}_p, \mathbf{E}_f$. For a measured data sequence of $\mathcal{N}$ samples the number of columns in the Hankel matrices is

$$N = \mathcal{N} - l_p - l_f + 1 \tag{5}$$

978-1-4799-8701-6/15/$31.00 ©2015 IEEE.

with l_p the past horizon and l_f the future horizon. For some steps in the algorithms the Hankel matrices are separated row-wise with notation

$$\mathbf{Y}_i = \begin{bmatrix} \mathbf{Y}_{f1} \\ \vdots \\ \mathbf{Y}_{fi} \end{bmatrix} = \mathbf{Y}_{p,i,N} \quad \text{for} \quad 1 \leq i \leq l_f \tag{6}$$

The Markov state of the k-th time step is

$$\boldsymbol{x}_k = \left(q\mathbf{I} - \bar{\mathbf{A}}\right)^{-1} \begin{pmatrix} \bar{\mathbf{B}} & \mathbf{K} \end{pmatrix} \begin{pmatrix} \boldsymbol{u}_k \\ \boldsymbol{y}_k \end{pmatrix} \tag{7}$$

with $\bar{\mathbf{A}} = \mathbf{A} - \mathbf{KC}$ and $\bar{\mathbf{B}} = \mathbf{B} - \mathbf{KD}$. When the state is expanded over a past horizon of p time steps the Markov state sequence is given by

$$\begin{aligned} \mathbf{X}_{p,N} &= [\boldsymbol{x}_p \;\; \boldsymbol{x}_{p+1} \;\; \dots \;\; \boldsymbol{x}_{p+N-1}] = \bar{\mathbf{A}}^p \mathbf{X}_{0,N} + \bar{\mathcal{K}} \mathbf{Z}_p \quad (8) \\ &\approx \bar{\mathcal{K}} \mathbf{Z}_p \quad (9) \end{aligned}$$

where

$$\bar{\mathcal{K}} = \left[\bar{\mathbf{A}}^{p-1}\bar{\mathbf{B}} \;\; \dots \;\; \bar{\mathbf{A}}\bar{\mathbf{B}} \;\; \bar{\mathbf{B}} \;\; \bar{\mathbf{A}}^{p-1}\mathbf{K} \;\; \dots \;\; \bar{\mathbf{A}}\mathbf{K} \;\; \mathbf{K}\right] \tag{10}$$

$$\mathbf{Z}_p = \begin{bmatrix} \mathbf{U}_p^T & \mathbf{Y}_p^T \end{bmatrix}^T \tag{11}$$

The algorithms use a bank of output predictors which is described in innovation form representation as

$$\mathbf{Y}_f \approx \boldsymbol{\Gamma}_f \bar{\mathcal{K}} \mathbf{Z}_p + \mathbf{H}_f \mathbf{U}_f + \mathbf{G}_f \mathbf{E}_f + \mathbf{E}_f \tag{12}$$

with the extended observability matrix

$$\boldsymbol{\Gamma}_f = \begin{bmatrix} \mathbf{C} \\ \mathbf{CA} \\ \vdots \\ \mathbf{CA}^{f-1} \end{bmatrix} \tag{13}$$

and the lower triangular block Toeplitz matrices which contain the Markov parameters of the system.

$$\mathbf{H}_f = \begin{bmatrix} \mathbf{D} & \mathbf{0} & \cdots & \mathbf{0} \\ \mathbf{CB} & \mathbf{D} & \cdots & \mathbf{0} \\ \vdots & \vdots & \ddots & \vdots \\ \mathbf{CA}^{f-2}\mathbf{B} & \mathbf{CA}^{f-3}\mathbf{B} & \cdots & \mathbf{D} \end{bmatrix} \tag{14}$$

$$\mathbf{G}_f = \begin{bmatrix} \mathbf{0} & \mathbf{0} & \cdots & \mathbf{0} \\ \mathbf{CK} & \mathbf{0} & \cdots & \mathbf{0} \\ \vdots & \vdots & \ddots & \vdots \\ \mathbf{CA}^{f-2}\mathbf{K} & \mathbf{CA}^{f-3}\mathbf{K} & \cdots & \mathbf{0} \end{bmatrix} \tag{15}$$

The main problem of the subspace identification is to get an estimate of $\boldsymbol{\Gamma}_f \bar{\mathcal{K}}$ as formulated in (12) and use this estimate to reconstruct a reduced order state sequence $\mathbf{X}_{p,N}$ as shown in (16) and (17). To get this sequence an order reduction step is performed via singular value decomposition and the optimal system order n is determined either by observing the dominant singular values or using an information criterion like the Akaike Information Criterion (AIC).

$$\widehat{\boldsymbol{\Gamma}_f \bar{\mathcal{K}}} \mathbf{Z}_p = \mathbf{U}\boldsymbol{\Sigma}\mathbf{V}^T \approx \mathbf{U}_n \boldsymbol{\Sigma}_n \mathbf{V}_n^T \tag{16}$$

After this the state sequence is constructed by using the first n right singular vectors.

$$\hat{\mathbf{X}}_{p,N} = \mathbf{V}_n^T \in \mathbb{R}^{n \times N} \tag{17}$$

Having constructed an estimate of the state sequence the system matrices can be estimated via least squares regression using the state sequence and the input/output data. For determination of the Kalman gain matrix the innovation sequence $\mathcal{E}_Y$ is estimated as the residuals of the solution of the system output equation (20).

$$\mathbf{Y}_{p,N-1} = \boldsymbol{\mathcal{Y}} = \underbrace{\begin{bmatrix} \hat{\mathbf{C}} & \hat{\mathbf{D}} \end{bmatrix}}_{\boldsymbol{\Theta}} \underbrace{\begin{bmatrix} \hat{\mathbf{X}}_{p,N-1} \\ \mathbf{U}_{p,N-1} \end{bmatrix}}_{\boldsymbol{\mathcal{W}}} + \boldsymbol{\mathcal{E}}_Y \tag{18}$$

$$\hat{\boldsymbol{\Theta}} = \boldsymbol{\mathcal{Y}} \boldsymbol{\mathcal{W}}^\dagger \tag{19}$$

$$\hat{\boldsymbol{\mathcal{E}}}_Y = \boldsymbol{\mathcal{Y}} \left(\mathbf{I} - \boldsymbol{\mathcal{W}}^\dagger \boldsymbol{\mathcal{W}}\right) \tag{20}$$

$$\hat{\mathbf{X}}_{p+1,N-1} = [\mathbf{A} \;\; \mathbf{B} \;\; \mathbf{K}] \begin{bmatrix} \hat{\mathbf{X}}_{p,N-1} \\ \mathbf{U}_{p,N-1} \\ \hat{\boldsymbol{\mathcal{E}}}_Y \end{bmatrix} \tag{21}$$

But under some conditions the Kalman gain obtained by (21) is not stabilizing the system. Therefore there is another approach to estimate the Kalman gain matrix by first estimating $\mathbf{A}$ and $\mathbf{B}$ with (22) and the sample covariance of the noise sequences with the least squares problem (23). In advance $\mathbf{K}$ can be computed by solving the discrete algebraic Riccati equation (24)-(25) which results in higher computational effort but guarantees a stabilizing Kalman gain.

$$\hat{\mathbf{X}}_{p+1,N-1} = [\mathbf{A} \;\; \mathbf{B}] \begin{bmatrix} \hat{\mathbf{X}}_{p,N-1} \\ \mathbf{U}_{p,N-1} \end{bmatrix} + \boldsymbol{\mathcal{E}}_X \tag{22}$$

$$\begin{bmatrix} \hat{\mathbf{Q}} & \hat{\mathbf{S}} \\ \hat{\mathbf{S}}^T & \hat{\mathbf{R}} \end{bmatrix} = \lim_{N \to \infty} \frac{1}{N-1} \begin{bmatrix} \boldsymbol{\mathcal{E}}_X \\ \boldsymbol{\mathcal{E}}_Y \end{bmatrix} [\boldsymbol{\mathcal{E}}_X \;\; \boldsymbol{\mathcal{E}}_Y] \tag{23}$$

$$\begin{aligned} \hat{\mathbf{P}} &= \hat{\mathbf{A}}\hat{\mathbf{P}}\hat{\mathbf{A}}^T + \hat{\mathbf{Q}} \\ &\quad - \left(\hat{\mathbf{S}} + \hat{\mathbf{A}}\hat{\mathbf{P}}\hat{\mathbf{C}}^T\right)\left(\hat{\mathbf{C}}\hat{\mathbf{P}}\hat{\mathbf{C}}^T\right)^{-1}\left(\hat{\mathbf{S}} + \hat{\mathbf{A}}\hat{\mathbf{P}}\hat{\mathbf{C}}^T\right)^T \quad (24) \end{aligned}$$

$$\hat{\mathbf{K}} = \left(\hat{\mathbf{S}} + \hat{\mathbf{A}}\hat{\mathbf{P}}\hat{\mathbf{C}}^T\right)\left(\hat{\mathbf{R}} + \hat{\mathbf{C}}\hat{\mathbf{P}}\hat{\mathbf{C}}^T\right)^{-1} \tag{25}$$

As stated before the main goal of subspace identification is to get an estimate of the $\boldsymbol{\Gamma}_f \bar{\mathcal{K}}$ to construct the Markov state and calculate the system matrices. In the following subsections three algorithms are explained which use different techniques to calculate $\widehat{\boldsymbol{\Gamma}_f \bar{\mathcal{K}}}$.

A. Single-stage procedure

The first algorithm explained is of the class of single-stage algorithms which solves only one linear least squares problem to estimate the Markov state sequence. First step is the estimation of a High-Order Auto-Regressive with eXogenous inputs (HOARX) model by performing a least squares regression of the first block-row of equation (12). Since there is either a delay in the controller or in the system the innovation $\mathbf{e}_k$ and the control input $\mathbf{u}_k$ are uncorrelated and the estimate is unbiased.

$$\mathbf{Y}_{f1} = \mathbf{Y}_{p,N} = \mathbf{C}\bar{\mathcal{K}}\mathbf{Z}_p + \mathbf{D}\mathbf{U}_{f1} + \mathbf{E}_{f1} \tag{26}$$

$$\left[\begin{array}{cc} \widehat{\mathbf{C}\bar{\mathcal{K}}} & \hat{\mathbf{D}} \end{array}\right] = \mathbf{Y}_{p,N} \left[\begin{array}{c} \mathbf{Z}_p \\ \mathbf{U}_{p,N} \end{array}\right]^{\dagger} \tag{27}$$

from $\mathbf{C}\bar{\mathcal{K}}$ and $\mathbf{D}$ one can get the Markov parameters of the predictor form description directly which are defined as

$$\Phi_\tau = \left[\begin{array}{cc} \Phi_\tau^{\bar{B}} & \Phi_\tau^{K} \end{array}\right] = \mathbf{C}\bar{\mathbf{A}}^{\tau-1} \left[\begin{array}{cc} \bar{\mathbf{B}} & \mathbf{K} \end{array}\right] \tag{28}$$

After converting the Markov parameters into innovation form representation an estimate of $\mathbf{\Gamma}_f\bar{\mathcal{K}}$ can be constructed referred to [10].

B. Double-stage procedure

This algorithm uses the solution of (27) to construct a pre-estimate of the Toeplitz matrix $\hat{\mathbf{H}}_f$ and substitute this into (12) to make the future input-output terms and the innovation uncorrelated.

$$\mathbf{Y}_{f^-} = \mathbf{Y}_f - \hat{\mathbf{H}}_f\mathbf{U}_f = \mathbf{\Gamma}\bar{\mathcal{K}}\mathbf{Z}_p + \mathbf{G}_f\mathbf{E}_f + \mathbf{E}_f \tag{29}$$

The new problem (29) is then solved by canonical variate analysis between $\mathbf{Y}_{f^-}$ and $\mathbf{Z}_p$.

$$\widehat{\mathbf{\Gamma}_f\bar{\mathcal{K}}} = \left(\mathbf{Y}_{f^-}\mathbf{Y}_{f^-}^T\right)^{-1/2} \cdot \mathbf{Y}_{f^-}\mathbf{Z}_p^T \cdot \left(\mathbf{Z}_p\mathbf{Z}_p^T\right)^{-1/2} \tag{30}$$

C. Multi-stage procedure

The third one is a multi-stage type algorithm based on the innovation estimation pre-estimate procedure of Qin and Ljung [8]. Here the bank of predictors (12) is solved row-wise for $i = 1 \ldots f$ which makes it the computationally less efficient one.

$$\mathbf{Y}_{fi} = \mathbf{\Gamma}_{fi}\bar{\mathcal{K}}\mathbf{Z}_p + \mathbf{H}_{fi}\mathbf{U}_i + \mathbf{G}_{fi}\hat{\mathbf{E}}_{i-1} + \mathbf{E}_{fi} \tag{31}$$

To get the estimate of $\mathbf{\Gamma}_f\bar{\mathcal{K}}$ the $\mathbf{\Gamma}_{fi}\bar{\mathcal{K}}$ are extracted out of each solution and stacked on top each other, then the state sequence and the system matrices can be estimated using (16)-(21).

$$\left[\begin{array}{ccc} \widehat{\mathbf{\Gamma}_{fi}\bar{\mathcal{K}}} & \hat{\mathbf{H}}_{fi} & \hat{\mathbf{G}}_{fi} \end{array}\right] = \mathbf{Y}_{fi} \left[\begin{array}{c} \mathbf{Z}_p \\ \mathbf{U}_i \\ \hat{\mathbf{E}}_{i-1} \end{array}\right]^{\dagger} \tag{32}$$

D. System order determination

For determination of the optimal system order the identification of the dominant singular values can be quite difficult. So the use of an information criterion can be helpful. The used information criterion is the AIC (33) developed by Akaike which computes the log likelihood function of the error and uses the number of estimated parameters M_n as a penalty term to prevent over fitting.

$$AIC(n) = -2\log p(\mathbf{Y}^N|\mathbf{U}^N, \hat{\boldsymbol{\theta}}(n)) + 2M_n \tag{33}$$

According to [7] the number of independent parameters for estimating a system model in state space representation is:

$$M_n = n(2l+m) + lm + \frac{l(l+1)}{2} \tag{34}$$

Since the AIC is designed for a large number of samples a correction term for a smaller number of samples is

$$f = \frac{N}{N - \frac{M_n}{n} + \frac{n+1}{2}} \tag{35}$$

According to [2] the calculation of the AIC is simplified to (36) for Gaussian distributed innovation e_k.

$$AIC(n) = N(l(1+\ln(2\pi)) + \ln|cov(\boldsymbol{\mathcal{E}}_Y)|) + 2M_n f \tag{36}$$

For the process described in the next chapter there is another method to determine the system order. Since the dynamical behavior of the mechanical multibody system can be explained by Newton's equations of motion one can easily obtain the true order of the system.

III. The two arm planar robot process

The benchmark process in this paper is a two arm planar robot shown in fig. 1. The robot consists of two links connected via two revolute joints. Each link is modeled as a rigid body and has an individual mass m_i and moment of inertia I_i with respect to its center of mass. The joints can be actuated externally through the torques τ_i and the joint position is given by the angles θ_i. If both links are in a straight line and parallel to the z-axis the joint angles are in zero position. l_1 and l_2 are the distances between the joint and the center of mass of the appropriate link, while a_1 is the length of the first link. For this example of a planar robot gravitation is acting along the negative z-axis.

A. Kinematics

The kinematics of this robot arm is described by (37) and (38) which are the x and z coordinates of each links center of mass with respect to the joint angles.

$$\boldsymbol{c}_1 = \left(\begin{array}{c} l_1\,\sin(\theta_1) \\ l_1\,\cos(\theta_1) \end{array}\right) \tag{37}$$

$$\boldsymbol{c}_2 = \left(\begin{array}{c} a_1\,\sin(\theta_1) + l_2\,\sin(\theta_1+\theta_2) \\ a_1\,\cos(\theta_1) + l_2\,\cos(\theta_1+\theta_2) \end{array}\right) \tag{38}$$

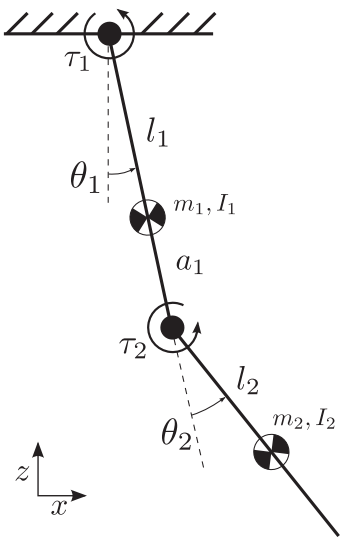

Fig. 1. Schematic of the two arm robot

B. Dynamics

The dynamics of this process are described by the nonlinear differential matrix equation (39). Where $\mathbf{M}(\boldsymbol{\theta})$ is the mass matrix of the system and $\mathbf{V}(\dot{\boldsymbol{\theta}}, \boldsymbol{\theta})$ is a nonlinear function containing the centrifugal, Coriolis and gravitational terms. The second term on the right hand side represents viscous friction acting against the motion. The determination of $\mathbf{M}$ and $\mathbf{V}$ is done via the Lagrangian dynamic formulation as described in [11] and [12]. For the used robot arm the exact dynamic equations are given in (40) - (46).

$$\mathbf{M}(\boldsymbol{\theta})\ddot{\boldsymbol{\theta}} + \mathbf{V}(\dot{\boldsymbol{\theta}}, \boldsymbol{\theta}) = \boldsymbol{\tau} - \mu\dot{\boldsymbol{\theta}} \tag{39}$$

$$\mathbf{M} = \begin{bmatrix} m_{11} & m_{12} \\ m_{21} & m_{22} \end{bmatrix} \tag{40}$$

$$\begin{aligned} m_{11} &= m_2\, {a_1}^2 + 2\, m_2\, \cos(\theta_2)\; a_1\, l_2 + m_1\, {l_1}^2 \\ &\quad + m_2\, {l_2}^2 + I_1 + I_2 \qquad (41) \\ m_{12} &= m_{21} = m_2\, {l_2}^2 + a_1\, m_2\, \cos(\theta_2)\; l_2 + I_2 \qquad (42) \\ m_{22} &= m_2\, {l_2}^2 + I_2 \qquad (43) \end{aligned}$$

$$\mathbf{V} = \begin{bmatrix} v_1 \\ v_2 \end{bmatrix} \tag{44}$$

$$\begin{aligned} v_1 &= -g\, m_2\; (a_1\, \sin(\theta_1) + l_2\, \sin(\theta_1 + \theta_2)) \\ &\quad -g\, l_1\, m_1\, \sin(\theta_1) \\ &\quad -\dot{\theta}_2\, a_1\, l_2\, m_2\, \sin(\theta_2)\; \left(2\,\dot{\theta}_1 + \dot{\theta}_2\right) \qquad (45) \\ v_2 &= -l_2\, m_2\, \left(g\, \sin(\theta_1 + \theta_2) - \dot{\theta}_1^2\, a_1\, \sin(\theta_2)\right) \qquad (46) \end{aligned}$$

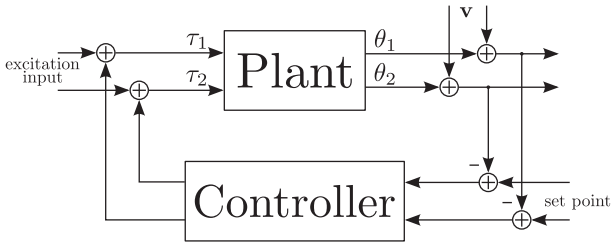

Fig. 2. Block scheme of the closed loop experiment

IV. Simulation Experiment

To test the described subspace identification algorithms the following experiment is built up. The plant is in closed-loop with two separate proportional controllers - one for each joint angle - which maintain different operating conditions. Since the algorithms identify linear models the plant is being linearized around the set point using the analytical description of the system dynamics in order to compare the identified solution to the real plant. Excitation of the plant is performed by two orthogonal PRBS sequences of period $M = 1023$ at the torque inputs simultaneously to identify the two by two MIMO process in one single experiment. Additive Gaussian noise $\mathbf{v}$ is added to the system outputs with zero mean and 0.1 variance. Further parameters are the sample time $T_s = 50$ms and the past and future horizons for the SSID algorithms with $l_p = l_f = 20$.

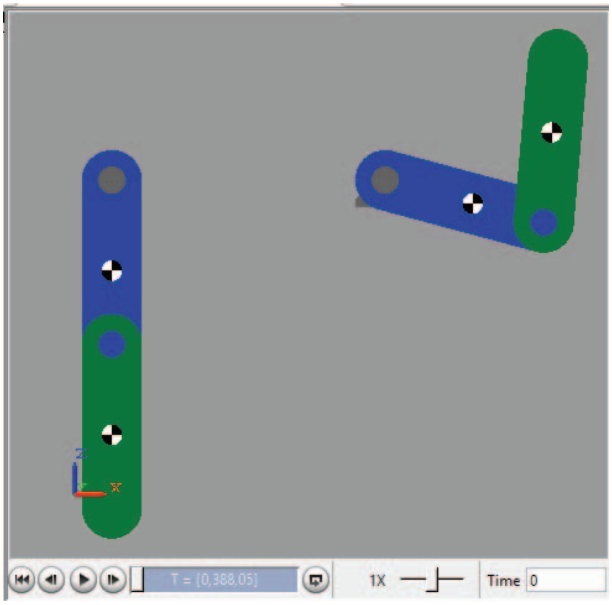

Fig. 3. Model of the robot arm in SimMechanics

Within this setup two experiments are chosen, first with a locally stable operating point and second with an unstable one. Simulation of the system is performed using Matlab/Simulink. Additionally the SimMechanics toolbox is used to model the robot arm. Figure 3 shows the robot arm with the chosen setpoints. The left one operates around $setpoint_1 = [0\ 0]$ degrees for θ_1 and θ_2 respectively and the right arm operates around $setpoint_2 = [75\ 100]$ degrees. Each experiment is executed 50 times with different initial values for the noise

generator.

To compare the system models identified by each algorithm with the real plant dynamics the dynamic equation (39) is linearized around the two setpoints and then the system matrices are discretized with the sample time T_s. The matrices $\mathbf{A}_1$ and $\mathbf{B}_1$ correspond to $setpoint_1$ and $\mathbf{A}_2$ and $\mathbf{B}_2$ correspond to $setpoint_2$. $\mathbf{C}$ and $\mathbf{D}$ are the same for both cases.

$$\mathbf{A}_1 = \begin{bmatrix} 0.9669 & 0.0105 & 0.0483 & 0.0020 \\ 0.0267 & 0.9537 & 0.0023 & 0.0440 \\ -1.2914 & 0.3854 & 0.9242 & 0.0808 \\ 0.9979 & -1.7636 & 0.0971 & 0.7569 \end{bmatrix}$$

$$\mathbf{B}_1 = \begin{bmatrix} 0.0011\text{e-}5 & -0.0019\text{e-}5 \\ -0.0019\text{e-}5 & 0.0052\text{e-}5 \\ 0.0427\text{e-}5 & -0.0703\text{e-}5 \\ -0.0703\text{e-}5 & 0.1967\text{e-}5 \end{bmatrix}$$

$$\mathbf{A}_2 = \begin{bmatrix} 0.9922 & 0.0016 & 0.0490 & 0.0008 \\ 0.0357 & 1.0275 & 0.0014 & 0.0477 \\ -0.3026 & 0.0687 & 0.9565 & 0.0322 \\ 1.4033 & 1.0837 & 0.0663 & 0.9185 \end{bmatrix}$$

$$\mathbf{B}_2 = \begin{bmatrix} 0.0009\text{e-}5 & -0.0008\text{e-}5 \\ -0.0008\text{e-}5 & 0.0028\text{e-}5 \\ 0.0356\text{e-}5 & -0.0307\text{e-}5 \\ -0.0307\text{e-}5 & 0.1090\text{e-}5 \end{bmatrix}$$

$$\mathbf{C} = \begin{bmatrix} 1 & 0 & 0 & 0 \\ 0 & 1 & 0 & 0 \end{bmatrix}, \mathbf{D} = \begin{bmatrix} 0 & 0 \\ 0 & 0 \end{bmatrix}$$

V. Simulation Results

To get an overview about the performance of the used subspace model identification algorithms the eigenvalues of each estimated system matrix are compared with the eigenvalues of the corresponding linearized system matrices. In this part of the experiment the system order for the SMI procedures to estimate is fixed to the analytically determined order $n = 4$. Figures 4-6 show the results of the Monte Carlo simulation for each algorithm in the two operating points. It can be seen that at the locally stable operating point two of the eigenvalues are well estimated whereas the other two have poor estimates. Further has the double stage algorithm higher variance in the estimate of each eigenvalue than the other algorithms.

At the second operating point where the system is locally unstable one can observe that each estimated eigenvalue has a certain distance to the corresponding eigenvalue of the linearized system. But the distribution of the estimates looks like the distribution of the true eigenvalues only with some offset. Remarkably is that each algorithm estimates the unstable eigenvalue of the system. As before the double stage algorithm has a higher variance in the estimates.

As a second measure of the quality of the identified models the coefficient of determination (47) is calculated and averaged over the 50 repetitions of each experiment for each of the two outputs y_i.

$$R^2 = 1 - \frac{\sum_{k=1}^{N}(y_i(k) - \hat{y}_i(k))^2}{\sum_{k=1}^{N}(y_i(k) - \bar{y}_i)^2} \tag{47}$$

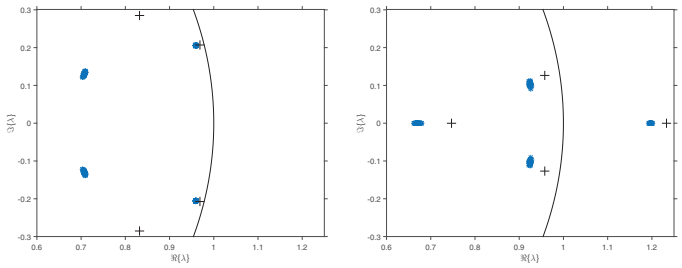

(a) (b)

Fig. 4. eigenvalues of the linearized system + and the system estimated by the single-stage procedure ∗ for experiment 1 (a) and for experiment 2 (b)

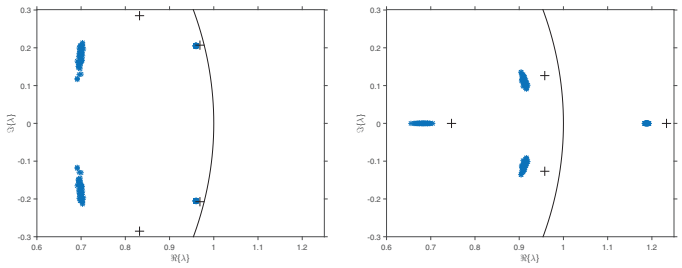

(a) (b)

Fig. 5. eigenvalues of the linearized system + and the system estimated by the single-stage procedure ∗ for experiment 1 (a) and for experiment 2 (b)

Tables I and II show the results of the model validation measurement for the two outputs in both operating points. For the first experiment one can observe that the estimate obtained by forcing the algorithm to use the true system order gives a better fit than the use of the AIC. Whereas in the second experiment the results are the other way around which could be explained through higher nonlinear effects in the operating region around $setpoint_2$. As shown in Fig. 7(a) the AIC optimal system order in experiment 1 is $n = 4$ in most of the simulation runs for each algorithm. Considering experiment 2 (Fig. 7(b)) the AIC optimal order is $n = 5$ for the single- and double-stage procedure and even $n = 6$ for the multi-stage method in order to cover the nonlinearities with a linear system model.

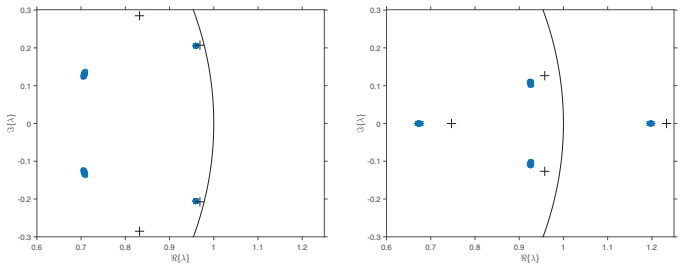

(a) (b)

Fig. 6. eigenvalues of the linearized system + and the system estimated by the single-stage procedure ∗ for experiment 1 (a) and for experiment 2 (b)

TABLE I. MEAN VAF VALUES OF EXPERIMENT 1

algorithm	true system order		AIC order estimate	
	output 1	output 2	output 1	output 2
single-stage	99.88	99.93	93.34	94.55
double-stage	99.53	98.96	99.08	96.84
multi-stage	99.91	99.74	98.19	92.43

TABLE II. MEAN VAF VALUES OF EXPERIMENT 2

algorithm	true system order		AIC order estimate	
	output 1	output 2	output 1	output 2
single-stage	98.08	99.55	99.90	99.96
double-stage	98.04	89.90	99.33	96.69
multi-stage	96.55	68.82	99.97	99.97

VI. CONCLUSION

In this paper we discussed several subspace state space identification methods and its application on actuated multi-body systems in closed loop control circumstances. The simulation results are encouraging. The ultimate goal of this work is to use the investigated identification methods for a real service robot. The identified models can be used for controller and observer tuning. Another idea is to use the methods for diagnostic purposes.

REFERENCES

[1] Larimore, W.E., *Canonical Variate Analysis in Identification, Filtering and Adaptive Control*, Proceedings of the 29th Conference on Decision and Control, Hawaii, 1990

[2] Peloubet, R.P. and Haller, R.L. and Bolding, R.M., *On-Line Adaptive Control of Unstable Aircraft Wing Flutter*, Proceedings of the 29th Conference on Decision and Control, Hawaii, 1990

[3] Verheagen, M. and Dewilde, P., *Subspace model identification, Part I: The output-error state space model identification class of algorithms*, Int. J. Control, Vol. 56, 1187-1210, 1992

[4] Van Overschee, P. and DeMoor, B., *Subspace Identification of Linear Systems: Theory, Implementation, Application*, Kluwer Academic Publischers, 1996

[5] Ljung, L. and McKelvey, T., *Subspace identification from closed loop data*, Signal Processing 52, 209-215, 1996

[6] Ljung, L., *System Identification: Theory for the user*, second ed., Prentice-Hall, Inc., 1999

[7] Larimore, W.E., *Automated Multivariable System Identification and Industrial Applications*, Proceedings of the American Control Conference, San Diego, California, 1999

[8] Qin, S.J. and Ljung, L., *Closed-loop Subspace Identification with Innovation Estimation*, Proceedings of SYSID 2003, Rotterdam, 2003

[9] Chiuso, A., *The role of Vector Auto Regressive Modeling in Predictor-Based Subspace Identification*, Automatica, Vol. 43, No. 6, 2007

[10] de Korte, R., *Subspace-Based Identification Techniques for a 'Smart' Wind Turbine Rotor Blade*, Delft University of Technology, M.Sc. Thesis, 2009

[11] Murray, R.M. and Li, Z. and Sastry, S.S., *A Mathematical Introduction to Robotic Manipulation*, CRC Press, 1994

[12] Craig, J.J., *Introduction to Robotics: Mechanics and Control*, third ed., Pearson Prentice Hall, 2005

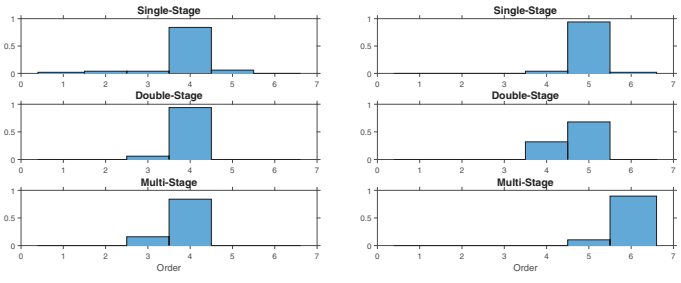

(a) (b)

Fig. 7. histogram of the order distribution obtained by the information criterion